Ultrasonics Sonochemistry 21 (2014) 1908–1915

Contents lists available at ScienceDirect

Ultrasonics Sonochemistry

journal homepage: www.elsevier.com/locate/ultson

Sonocrystallization and sonofragmentation

John R.G. Sander, Brad W. Zeiger, Kenneth S. Suslick *

Department of Chemistry, University of Illinois at Urbana-Champaign, 600 S. Mathews Av., Urbana, IL 61801, USA

ARTICLE INFO

Article history:
Received 20 December 2013
Received in revised form 5 February 2014
Accepted 6 February 2014
Available online 20 February 2014

Keywords:
Ultrasound
Sonocrystallization
Sonofragmentation
Sonochemistry
Cavitation
Nucleation

ABSTRACT

The application of ultrasound to crystallization (i.e., sonocrystallization) can dramatically affect the properties of the crystalline products. Sonocrystallization induces rapid nucleation that generally yields smaller crystals of a more narrow size distribution compared to quiescent crystallizations. The mechanism by which ultrasound induces nucleation remains unclear although reports show the potential contributions of shockwaves and increases in heterogeneous nucleation. In addition, the fragmentation of molecular crystals during ultrasonic irradiation is an emerging aspect of sonocrystallization and nucleation. Decoupling experiments were performed to confirm that interactions between shockwaves and crystals are the main contributors to crystal breakage. In this review, we build upon previous studies and emphasize the effects of ultrasound on the crystallization of organic molecules. Recent work on the applications of sonocrystallized materials in pharmaceutics and materials science are also discussed.

1. Introduction

The application of ultrasound to crystallizations has afforded substantially improved access to a wide variety of crystalline materials, but the mechanisms of action of the ultrasound remain ambiguous. The chemical and physical effects of ultrasound do not come from any direct interaction with molecular species. Instead, sonochemistry arises from acoustic cavitation: the formation, growth, and implosive collapse of bubbles in a liquid [1–4]. In homogeneous liquids, collapse of bubble clouds produces intense local heating with a temperature of ~5000 K, pressures of ~10^5 kPa, and enormous heating and cooling rates above 10^{10} K/s within isolated sub-micron reactors [5–11]. The physical effects of ultrasound that arise in heterogeneous, solid–liquid systems are also derived from cavitation. When a cavitating bubble (i.e., ~50 μm at maximum size under 20 kHz ultrasound) collapses in the presence of a significantly larger surface, the bubble undergoes a markedly asymmetric collapse, which generates a high-speed jet of liquid with a velocity >100 m/s that smashes into the surface [12,13]. The impingement of this jet can cause localized erosion, surface pitting, ultrasonic cleaning, and enhancement of surface chemistry [13]. Cavitational collapse also releases shockwaves that have velocities as high as ~4000 m/s and high pressure amplitudes of 10^6 kPa, which can easily produce plastic deformation of malleable metals and induce high velocity collisions between micron-sized solid particles [14–16].

In 1927, Richards and Loomis reported the first examination of the effects of ultrasound on crystallization (i.e., sonocrystallization) [17], but found only limited results. Supersaturated solutions and supercooled melts were "little affected" by ultrasonic irradiation, or yielded inconsistent results. The scientific literature on sonocrystallization remained relatively dormant until revitalization in the 1950s and 1960s when many of the benefits of sonocrystallization discussed in current literature were first observed. Kapustin, for example, reviewed work by colleagues within the former Soviet Union that emphasized the reduction of grain size in melt crystallizations via ultrasound [18]. Turner et al. reported that a short burst of high intensity ultrasound induced crystallization of sugar syrups that were normally resistant to crystallization [19]. Several other labs reported that micronized, uniform crystals of pharmaceutical agents were also achieved via ultrasound-based approaches [20–22]. Over fifty years have passed since early reviews on sonocrystallization discussed proposed mechanisms of action [22,23]. The desire to understand the fundamentals of this process and control the outcome of sonocrystallization has been a driving force in the field. In this review, we build upon previous studies and emphasize the effects of ultrasound on the crystallization of organic molecules [24–29]. The current views on the mechanisms of action of ultrasound will be discussed along with the strides made towards optimizing sonocrystallization to achieve a desired product. The impact of sonofragmentation on molecular crystals will also be discussed. Additionally, the review highlights recent applications of sonocrystallization products.

* Corresponding author. Tel.: +1 217 333 2794; fax: +1 217 244 3186.
E-mail address: ksuslick@illinois.edu (K.S. Suslick).

http://dx.doi.org/10.1016/j.ultsonch.2014.02.005
1350-4177/

2. Effects of ultrasound on crystallization

2.1. Induction time and metastable zone width

Interest in ultrasound effects on crystallization largely originates from reports that ultrasound can induce crystal nucleation. The challenge in translating experimental results into mechanistic insight lies in the inherent complexity of crystal nucleation, a field of active experimental and theoretical research [30,31]. Variations in crystal nucleation are generally analyzed by measuring the induction time and metastable zone width. Induction time is defined as the elapsed time between the achievement of supersaturation and the formation and detection of crystals [32], as illustrated in Fig. 1. The solution concentration remains relatively constant during this latency period until wide spread crystal growth occurs and rapidly relieves the supersaturation. Induction time measurements are greatly influenced by agitation, impurities, solution viscosity, degree of supersaturation, and the cooling rate (in any polythermal method of crystallization). In addition, the induction time is dependent on the method used to detect crystallization. The techniques employed vary from visual observations to analytical techniques that utilize conduction measurements or laser light scattering.

A number of groups have explored the induction time for organic molecules in the presence of ultrasound [33–35]. Among them, Guo and coworkers investigated the induction time of roxithromycin in antisolvent crystallization [34]. Starting from an acetone solution of roxithromycin, water (i.e., the antisolvent) was rapidly added to the solution and monitored for the onset of nucleation using laser light scattering. In the case of sonocrystallization experiments, water was added while simultaneously sonicating the solution. In the absence of ultrasound, the induction time of roxithromycin decreased with increasing supersaturation as expected. When ultrasonic irradiation is employed the induction time decreases significantly for all supersaturations (Fig. 2). From a detailed analysis, the authors conclude that it is an acceleration in diffusion in the presence of ultrasound that causes the reduction in induction times.

The ability of ultrasound to induce primary nucleation, and the possibility of a threshold energy input, was investigated by Miyasaka and coworkers [35–37]. In an initial investigation, acetylsalicylic acid solutions were supercooled and then exposed to ultrasonic irradiation with a titanium probe operating at

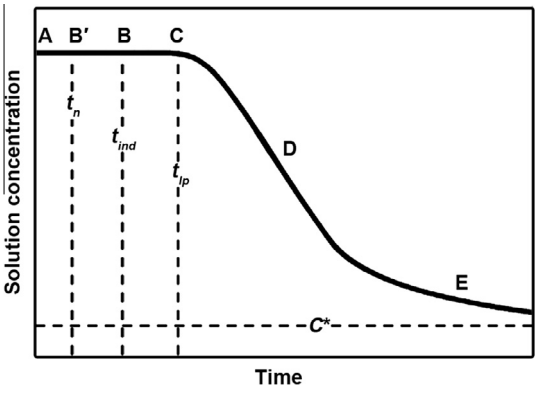

Fig. 1. Crystallization from a point of supersaturation (point A) followed by a lag time before crystal nucleation (point B′). The initial nuclei continue to grow until crystals reach a detectable size (point B). The solution concentration remains relatively constant (point C) then crystal growth rapidly reduces solution concentration (region D) until reaching equilibrium (region E). C^* = equilibrium saturation, t_n = nucleation time, t_{ind} = induction time, t_{lp} = latent period. Reprinted with permission from Ref. [32]. Copyright 2001 Elsevier.

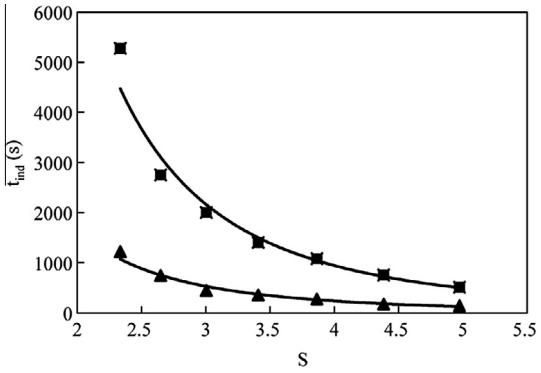

Fig. 2. Roxithromycin crystallization induction time (t_{ind}) versus the degree of supersaturation (S) in the absence (squares) or presence (triangles) of ultrasound (20 kHz). Reprinted with permission from Ref. [34]. Copyright 2004 Elsevier.

20 kHz for variable times and powers. Optical microscopy was used to determine the number of crystals formed after primary nucleation and the total number of crystals after 72 h. In these results, a low amount of ultrasonic energy (i.e., <100 J) was found to inhibit crystal nucleation when compared to crystallization performed in the absence of ultrasound. When a threshold of ultrasonic energy was reached, an induction period was no longer necessary to form stable nuclei and further increases in the ultrasonic energy input had little effect. By showing a correlation between the parameters, it is proposed that ultrasonic irradiation supplies the energy for primary nucleation. In a similar study, the induction time of *L*-serine and *L*-arginine showed that the induction time to crystallization decreases as ultrasonic power increases up to a limiting threshold value (Fig. 3) [35].

The MZW is defined as the region between an equilibrium saturation curve and the experimentally observed point of supersaturation when nucleation (and hence crystallization) occurs spontaneously. As an undersaturated solution is cooled, it will reach its equilibrium saturation point at some temperature T_0, but crystals generally will not form until some lower temperature at which point the solution is supersaturated. As the solution is cooled further, crystals will be observed at a limiting lower temperature T_{lim}. The MZW is simply defined as T_0–T_{lim}. Although the MZW is affected by a number of variables (e.g., presence of impurities, seeded microcrystals, rate of cooling, etc.), the experimentally determined value of MZW is a useful determination of the amount a solution can be cooled below its equilibrium saturation limit before nucleation occurs (Fig. 4) [38].

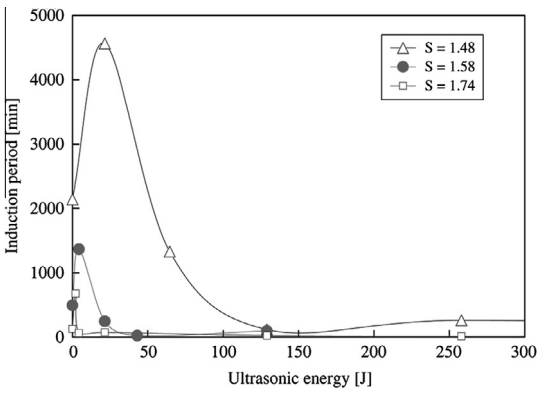

Fig. 3. Effect of ultrasonic power on the induction time of *L*-arginine at increasing supersaturation levels (S). Reprinted with permission from Ref. [35]. Copyright 2009 Elsevier.

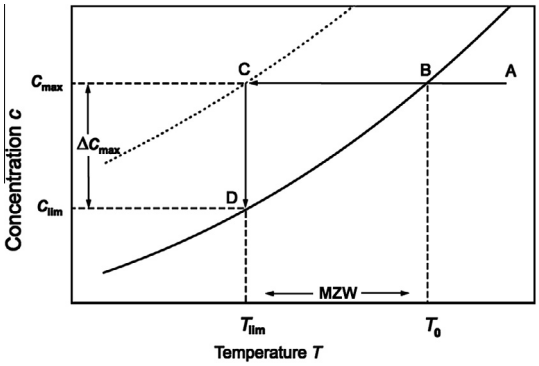

Fig. 4. Solubility as a function of temperature. The solid line represents the equilibrium saturation of a dissolved species in solution. For an initially undersaturated solution (point A with a concentration, C_{max}), as we cool the solution, it will reach its saturation point at temperature T_0 (point B), but crystals generally will not form until some lower temperature at which point the solution is supersaturated. As the solution is cooled further, crystals will be observed at a limiting lower temperature T_{lim} (point C). Crystal growth continues until the solution concentration reaches the equilibrium solubility curve (point D). The metastable zone width (MZW) is defined as T_0–T_{lim} for a polythermal crystallization. Reprinted with permission from Ref. [38]. Copyright 2009 Elsevier.

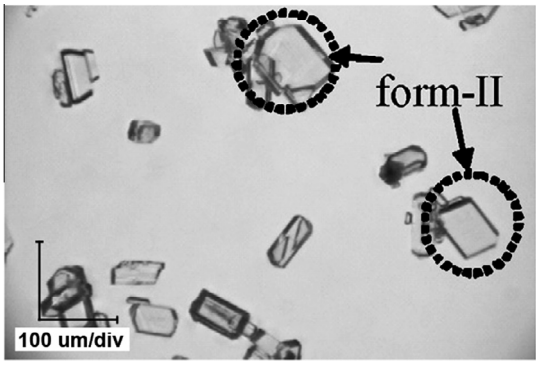

Fig. 5. Optical micrograph showing both sulfamerazine polymorphs (Form-I and Form-II) grew when ultrasound is applied during crystallization. Reprinted with permission from Ref. [42]. Copyright 2008 Elsevier.

A decrease in the MZW is often noted as a significant advantage afforded by sonocrystallization. The supersaturation level employed during crystallization affects purity, morphology, crystal size, and crystal size distribution. Sugars and sugar derivatives provide an example of the advantages observed when the MZW is reduced [39]. In the absence of ultrasound, sorbitol hexaacetate crystallizes as small, irregular crystals that are agglomerated. Repeating the same cooling crystallization, this time with ultrasonic irradiation, caused crystallization at 36.8 °C versus crystallization at 33.2 °C in the absence of ultrasound. Optical micrographs of the sonocrystallized sorbitol hexaacetate revealed large crystals with a well-defined morphology. Improved crystals are attributed to crystallization at a lower supersaturation, which favors slow, controlled, crystal growth.

Reduced induction times and MZWs have also been exploited in the controlled crystallization of polymorphs. Rasmuson and colleagues reported *p*-aminobenzoic acid polymorphs were selectively crystallized by adjusting the supersaturation and employing ultrasound [40]. The *p*-aminobenzoic acid polymorphs are enantiotropic and exhibit a transition temperature of ~25 °C, above which the α-polymorph is energetically favored. Sonocrystallization of *p*-aminobenzoic acid significantly reduced the induction time, narrowed the MZW, and reproducibly yielded pure crystals of the β-polymorph below the transition temperature. Interestingly, the β-polymorph was crystallized above 25 °C when ultrasound was used in combination with a low initial supersaturation. Ultrasound was hypothesized to influence the intermolecular interaction between molecules at the clustering phase prior to nucleation, thus, altering the polymorphic outcome of sonocrystallization. The effects of ultrasound on polymorphism have been reported for additional molecular crystals [41–43]. In the case of sulfamerazine, ultrasound was used to promote the formation of the Form-II polymorph (i.e., the stable polymorph below 51–54 °C) [42]. In the absence of ultrasound, Form-I crystallizes from a supersaturated solution and, despite extended suspension in acetonitrile, shows little conversion to the thermodynamically stable Form-II. Ultrasonic irradiation promoted the nucleation of Form-II from supersaturated solutions and expedited the conversion of Form-I suspensions to Form-II (Fig. 5). In a related study, specific lots of sulfamerazine Form-I failed to undergo phase transformation despite suspension for two weeks in acetonitrile, a strategy previously shown to be highly successful [44]. An acetyl derivative of sulfamerazine (i.e., N_4-acetylsulfamerazine) was identified as an impurity in the commercial lots that inhibited the transition from Form-I to Form-II. It would be interesting to determine if N_4-acetylsulfamerazine was present in the ultrasound-assisted experiments and if ultrasonic irradiation can overcome the inhibitory effects of impurities in polymorphic conversions.

2.2. Nucleation rate

Nucleation rate is a crucial parameter to optimize when the goal is production of small crystals (few micron- or nanometer sized), as high nucleation rates will generally yield small crystals in large numbers, rather than slower growth of fewer large crystals. Thus, as will be further discussed later in the review, an optimized nucleation rate can be crucial when striving for nanocrystals with a narrow size distribution. Dave and coworkers have investigated the nucleation rate of pharmaceutical agents (PAs) during antisolvent sonocrystallization and related the final crystal size and distribution to the nucleation rate [45–47]. Using a T-shaped experimental rig to optimize the mixing of solution and antisolvent, five PAs were precipitated and the classical theory of homogeneous nucleation was used to derive nucleation rates [47]. While a high nucleation rate resulted in smaller particles, an increase in supersaturation did not necessarily yield an increase in nucleation rate. Solvent polarity, specifically PA–solvent interactions, was shown to be an important parameter in determining nucleation rate, and thus, the crystal size in antisolvent sonocrystallization.

3. Optimization of sonocrystallization: process parameters, ultrasound variables, and mechanistic insights

3.1. Process parameters

The impetus for many sonocrystallization studies has been to crystallize monodisperse PAs of a particular size. Reducing the size of PA-based crystals to micro- and nanometer dimensions offers the potential to improve the physicochemical properties of a PA (i.e., dissolution rate) via non-covalent processes. The attributes of sonocrystallization (i.e., narrow MZW, high nucleation rate) contribute to an ability to induce rapid, widespread, nucleation followed by uniform crystal growth to obtain small crystals with a narrow size distribution. To achieve minimum crystal size and distribution researchers have focused on optimizing solvent choice, supersaturation, solvent-to-antisolvent ratio, and crystallization temperature; ultrasonic parameters are also critical here, and include power, frequency, and exposure time, but also the

experimental configuration of the ultrasonic irradiation (e.g., horn vs. bath vs. flow-through cell, etc.).

For instance, Hatkar and Gogate investigated the effects of process parameters on the antisolvent crystallization of salicylic acid [48]. The results showed the particle size was reduced when increasing solution concentration, sonication time, power, and when an ultrasonic horn was used instead of an ultrasonic bath. Over the temperature range of 25–35 °C the particle size remained constant whereas an increase in the solution injection rate yielded larger crystals with an increased aspect ratio. Similar optimization of sonocrystallization has been explored for molecules such as adipic acid [49,50], lactose [51–57], sirolimus [58–60], roxithromycin [34,61], and carbamazepine [62]. In the case of multi-component solids, MacGillivray and coworkers reported the sonochemical preparation of nano-cocrystals based on a pharmaceutical cocrystal [63]. A combination of multiple-solvents and surfactant were used in antisolvent sonocrystallization to overcome the solubility disparity of the cocrystal components (Fig. 6).

3.2. Mechanistic insights

The origin of sonocrystallization benefits has been the subject of speculation for over 50 years, with several proposed mechanisms that cite different sources for increased nucleation [23]. As previously mentioned, ultrasound induces acoustic cavitation in liquids, which simultaneously creates high local temperatures and pressure, produces shockwaves in the liquid, and generates foreign particles from erosion (e.g., of ultrasonic horns or of irradiated container surfaces); such multiple effects have prevented effective interpretation of the mechanism of sonocrystallization. The effects of convection on nucleation during sonication was the subject of a recent report by Nalajala and Moholkar in which experimental work was compared to simulations of bubble dynamics [64]. The components of convection modeled included microturbulence of the liquid, caused by the radial motion of cavitation bubbles, and shockwaves. The results show shockwaves increase the nucleation rate by an order of magnitude, possibly due to an increase in local concentration of solute molecules in the shock, whereas microturbulence effects on crystal growth were similar to mechanical stirring.

A recent report utilized high frequency sonocrystallization (i.e., 44–645 kHz), via plate transducers, to crystallize sodium chloride in the absence of the localized intense shear and turbulence inherently associated with an ultrasonic horn (e.g., 20 kHz) [65]. The ability to achieve a similar crystal size and distribution regardless of the frequency used suggests the high shear and mixing caused by an ultrasonic horn operating at 20 kHz may not be required (Fig. 7). High frequency ultrasound (e.g., 200 kHz to 2 MHz) also shows an ability to induce nucleation of molecular crystals, enhance crystal growth and uniformity, and hasten polymorphic conversion [66–68]. For example, sonocrystallization of adipic acid using 355.5 kHz irradiation yielded a narrower MZW and crystal size distribution than experiments performed with 204 and 610 kHz [67]; similarly, a recent paper by Nii and Takayanagi find improvements at 1.6 MHz compared to 20 kHz. The effect of frequency in these experiments is complicated, however, and may represent the relative efficiency of the individual experimental configurations (e.g., number of cavitation events per cc per sec for a given reactor set-up) rather than an intrinsic effect of frequency.

Induced nucleation via sonocrystallization is also believed to result from an increase in heterogeneous nucleation. Schembecker and coworkers utilized gassing experiments as a means to evaluate the surface of cavitation bubbles as potential nucleation sites [67,69–71]. In a comparison of ultrasound and gas sparging, both techniques were shown to reduce the MZW and affect the crystal size distribution. Similarly, Lyczko and colleagues speculated the existence of a segregation effect of a cavitation bubble that might promote nucleation by concentrating solute clusters on the bubble surface and act as a cluster attachment reactor [72]. An additional mechanism of action proposes that localized heating and cooling rates cause confined regions of increased supersaturation and that cavitation events somehow supply the energy necessary to overcome the energetic barrier to nucleation [27].

4. Sonofragmentation

The impact of ultrasound on molecular crystals plays a central role in sonocrystallization. Despite the immense interest in sonocrystallization, the effect of crystal breakage (i.e., sonofragmentation) on the product of sonocrystallization experiments remains comparatively unexplored. Suslick and coworkers reported the first studies of the effects of high intensity ultrasound on slurries of metallic nanoparticles [15,16]. The shockwaves created in the liquid by cavitation drive interparticle collisions in the slurry at sufficient speeds to cause intense localized heating, plastic deformation, spot-welding or melting of relatively low-melting point metals (e.g., Zn, Ni), but not refractory metals (e.g., W). Achieving a velocity that causes localized melting and agglomeration requires the metal particles to have a specific range of radii (i.e., a few microns): too small and they are unlikely to collide, too big and they are too difficult to accelerate. Literature reports on the mechanical attrition of molecular crystals in an ultrasound field also attribute crystal breakage to interparticle collisions, however, the intrinsic differences between molecular crystals and metallic nanoparticles (e.g., tensile strength) suggests the need for a detailed examination of molecular crystal breakage.

Recently, Zeiger and Suslick reported a series of experiments that evaluate the contributions of four potential sources of sonofragmentation: interparticle collisions, particle-horn collisions, particle-wall collisions, or particle–shockwave interactions [73].

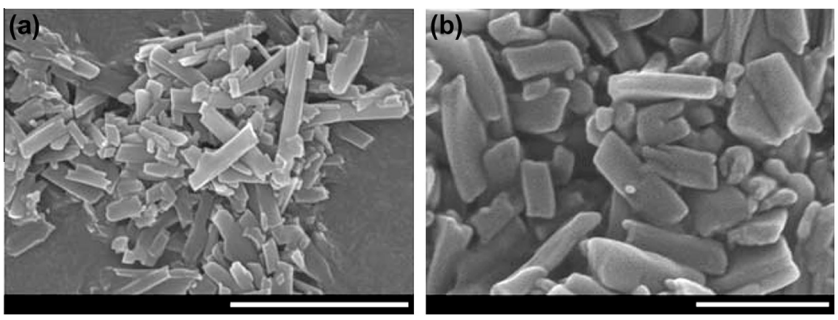

Fig. 6. Scanning electron micrographs revealing the caffeine 2,4-dihydroxybenzoic acid monohydrate cocrystal prepared using (a, scale bar 3 μm) a single solvent approach and (b, scale bar 500 nm) a two solvent approach. Reprinted with permission from Ref. [63]. Copyright 2010 WILEY-VCH Verlag GmbH & Co. KGaA, Weinheim.

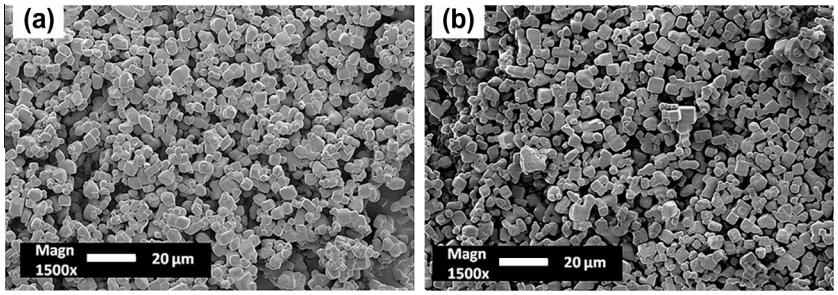

Fig. 7. Scanning electron micrographs showing sodium chloride crystals prepared using (a) a 20 kHz ultrasonic horn and (b) 500 kHz plate transducers. Reprinted with permission from Ref. [65]. Copyright 2013 Elsevier.

Aspirin crystals suspended in dodecane (as the antisolvent) were exposed to high intensity ultrasound at 10 W and 20 kHz using a titanium horn. Cross-polarized optical micrographs revealed the breakage of aspirin crystals (Fig. 8). The contribution of interparticle collisions to aspirin breakage was evaluated by varying the loading of aspirin crystals within the suspension. The average particle size after sonication lacked a dependence on aspirin loading, which suggests interparticle collisions are not a dominating contribution to sonofragmentation. To determine the contributions of particle-horn and particle-wall collisions to sonofragmentation, thin membranes were used to shield the suspensions from contact. Despite isolation, aspirin crystals continued to undergo breakage during sonication, in fact, when isolated from the vessel wall aspirin crystals experienced greater breakage due to the close proximity to the cavitation zone. Further evidence that particle-wall and particle-horn collisions are at best minor contributors was obtained by varying the size of the sonofragmentation reactor (Fig. 9). The minor change in particle size after sonication reaffirms that direct particle–shockwave interactions are the main contributor to the sonofragmentation of molecular crystals. We anticipate the impact of sonofragmentation on crystal morphology will play a more prominent role in the design of sonocrystallization experiments due to the effect of crystal morphology on properties such as filterability.

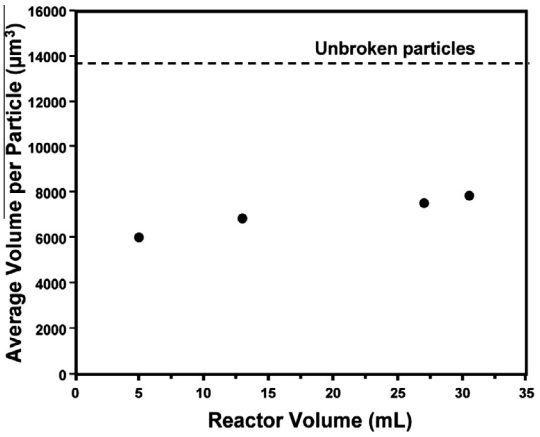

Fig. 9. Size of aspirin crystals after sonication for 30 s at 10 W using a constant loading of 0.01 g/mL. The reactor volume was increased over a 6-fold range. In addition, the distance between the ultrasonic horn and reactor wall was changed from 1.0 to 2.4 cm. Reprinted with permission from Ref. [73]. Copyright 2011 American Chemical Society.

5. Applications

A wide range of interesting materials can be obtained utilizing a sonocrystallization approach. Of special interest, sonocrystallization offers an alternative strategy to synthesize nanocrystalline PAs. Preparation of PA-based nanocrystals offers a non-covalent means to increase bioavailability due to the inherent properties of nanocrystals (e.g., surface area to volume ratio) [74]. PA-based nanocrystals have recently found utility in the field of inhalable drugs. Inhalable medicine is generally formulated with an aerodynamic radius of 1-2 µm to achieve deep-lung deposition [75]; however, Berkland and coworkers showed flocculated nanocrystals can attain the desired aerodynamic radius with the added advantages of improved kinetics of solubilization, facile aerosol formation, and improved bioavailability [76–79]. Antisolvent sonocrystallization in the presence of surfactant was utilized to prepare nanoparticles of budesonide. The nanosuspensions then underwent controlled flocculation with *L*-leucine to achieve a desired aerodynamic radius [76]. Similarly, sonocrystallization and spray drying were coupled to obtain crystals of salbutamol sulfate with a suitable aerodynamic radius for pulmonary delivery [80].

The effect of ultrasound on chirality also has potential implications in the pharmaceutical industry. In a controversial paper, Chen and coworkers reported that crystallization of $NaClO_3$ during

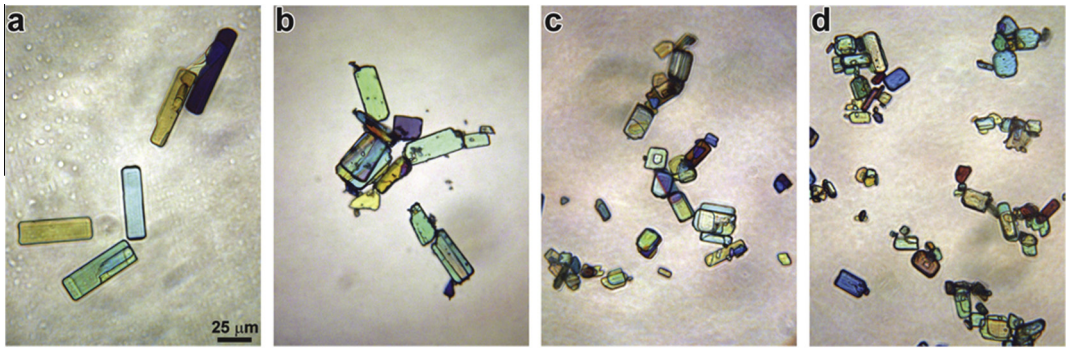

Fig. 8. Cross-polarized optical micrographs revealing the effects of high intensity ultrasound (i.e., 10 W, 20 kHz) (a) before sonication then after irradiation for (b) 1 min, (c) 3 min, and (d) 10 min. The micrographs were captured at the same magnification. Reprinted with permission from Ref. [73]. Copyright 2011 American Chemical Society.

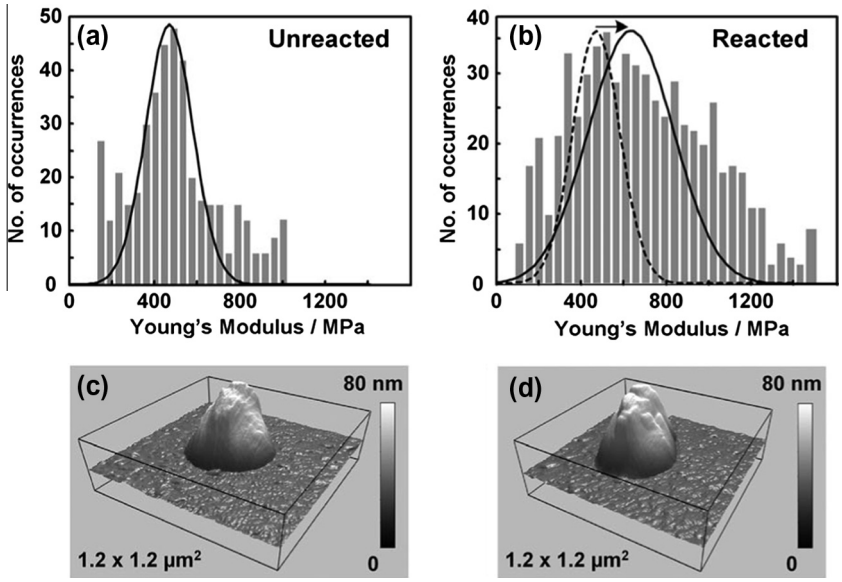

Fig. 10. Young's moduli for the 5-cyanoresorcinol *trans*-1,2,-bis(4-pyridyl)ethylene cocrystal (a) before and (b) after photoreaction. (c) AFM height measurement on a single nano-cocrystal and (d) height profile of the same crystal after 60 s of UV irradiation. Reprinted with permission from Ref. [85]. Copyright 2011 WILEY-VCH Verlag GmbH & Co. KGaA, Weinheim.

exposure to ultrasonic irradiation can break chiral symmetry [81]. Although cavitation is not expected to bias the chirality of crystallizations, an increase in secondary nucleation could be promoted [82]. In fact, follow up experiments revealed the enantiomeric excess of the product depended on the time interval between primary nucleation and the introduction of seeds with a particular handedness. A short time interval between primary nucleation and seeding lead to products with a high enantiomeric excess which supports chiral symmetry breaking via ultrasound is a self-seed inducing effect [83].

MacGillivray and colleagues utilized sonocrystallization to study changes in mechanical properties when cocrystals are reduced to nanometer-scale dimensions [84,85]. Originally low-intensity ultrasound was employed to synthesize nano- and micro-sized cocrystals of *trans*-1,2,-bis(4-pyridyl)ethylene and resorcinol. Scanning electron microscopy micrographs revealed that after exposure to UV irradiation the nano-cocrystals remained intact while larger crystals fractured [84]. The mechanical properties of nano-cocrystals were further examined using atomic force microscopy (AFM) [85]. In this instance, 5-cyanoresorcinol was used to arrange the reactive olefins such that a single-crystal-to-single-crystal photoreaction was observed in millimeter and nano-scale cocrystals. AFM was utilized to calculate the Young's moduli of millimeter-sized crystals before and after UV irradiation. The results showed the crystals became less stiff after photoreaction. Alternatively, the Young's modulus of nano-cocrystals after UV irradiation increased from 250 to 460 MPa which represents an 85% increase in crystal stiffness (Fig. 10).

In another application of sonocrystallization to prepare nano-cocrystals, Yan and coworkers synthesized stilbene-based nano-cocrystals that exhibit size dependent photoemission properties [86]. Initial attempts to synthesize the cocrystal via milling yielded aggregated particles with a broad size distribution; however, anti-solvent sonocrystallization successfully formed well-dispersed nano-cocrystals. The nano-cocrystals exhibit one- and two-phonon emission and fluorescence lifetimes that are distinct when compared to macro-sized cocrystals. In addition, the fluorescence spectra of the nano-cocrystals are temperature dependent and reversible within a temperature range, which has potential applications as thermosensitive materials (Fig. 11).

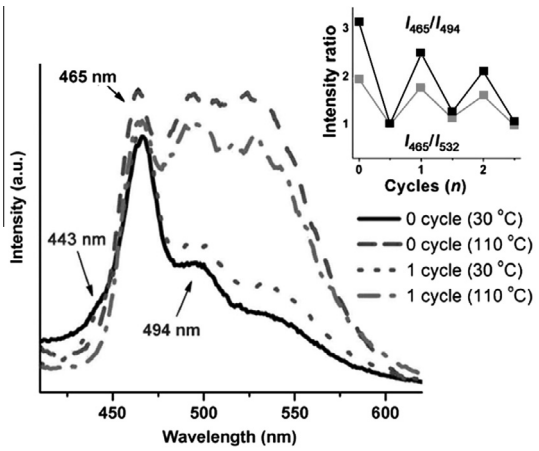

Fig. 11. Fluorescence spectra of a stilbene-based nano-cocrystal over two heating/cooling cycles. Inset shows the intensity ratio at I_{465}/I_{494} and I_{465}/I_{532} over three consecutive cycles. Reprinted with permission from Ref. [86]. Copyright 2013 WILEY-VCH Verlag GmbH & Co. KGaA, Weinheim.

6. Conclusions

Sonocrystallization has become a prominent method to prepare organic crystals with a desired size and size distribution. Ultrasound provides a means of reducing the induction time and MZW and of dramatically increasing the nucleation rate in crystallization experiments. The modification of crystallization parameters yields micro- and nanometer-sized crystals that are of particular interest to the pharmaceutical industry due to the increase in bioavailability associated with particle size reductions. The literature contains a wealth of reports that establish empirical control over sonocrystallization parameters (e.g., solution concentration) to achieve monodisperse crystals of a minimal size. The mechanism of action attributed to sonocrystallization, however, continues to be unclear. Recent gassing experiments and simulations of bubble dynamics suggest heterogeneous nucleation and

shockwaves increase crystal nucleation. The impact of crystal breakage during ultrasonic irradiation will continue to be of interest especially in the design of sonocrystallization experiments with prolonged sonication times (i.e., >3 min). The exploitation of PA-based nanocrystals in the pharmaceutical industry is expected to grow substantially, and thus, the ability of sonocrystallization to serve as a bottom-up route towards nanocrystals will continue to generate great interest. Recent reports show the material properties of organic crystals (e.g., hardness and solid-state luminescence) can exhibit distinct, advantageous behavior even at sizes of hundreds of nanometers. The continued expansion of sonocrystallization applications will be greatly benefited by the development of new technologies, including processes that couple atomization and ultrasound to produce crystals with well-defined size distributions and surfaces [87,88].

Acknowledgment

We gratefully acknowledge the financial support of the U.S. National Science Foundation (DMR-1206355).

References

[1] K.S. Suslick (Ed.), Ultrasound, Its Chemical, Physical, and Biological Effects, VCH Publishers Inc, New York, 1988.
[2] T.G. Leighton, The Acoustic Bubble, Academic Press, San Diego, 1994.
[3] T.J. Mason, J.P. Lorimer, Applied Sonochemistry: The Uses of Power Ultrasound in Chemistry and Processing, Wiley-VCH, Weinheim, 2001.
[4] Pankaj, M. Ashokkumar (Eds.), Theoretical and Experimental Sonochemistry Involving Inorganic Systems, Springer-Verlag Berlin, Berlin, 2011.
[5] K.S. Suslick, D.J. Flannigan, Inside a collapsing bubble: sonoluminescence and the conditions during cavitation, Annu. Rev. Phys. Chem. 59 (2008) 659–683.
[6] E.B. Flint, K.S. Suslick, The temperature of cavitation, Science 253 (1991) 1397–1399.
[7] W.B. McNamara, Y.T. Didenko, K.S. Suslick, Sonoluminescence temperatures during multi-bubble cavitation, Nature 401 (1999) 772–775.
[8] D.J. Flannigan, K.S. Suslick, Plasma formation and temperature measurement during single-bubble cavitation, Nature 434 (2005) 52–55.
[9] N.C. Eddingsaas, K.S. Suslick, Evidence for a plasma core during multibubble sonoluminescence in sulfuric acid, J. Am. Chem. Soc. 129 (2007) 3838–3839.
[10] H.X. Xu, N.C. Eddingsaas, K.S. Suslick, Spatial separation of cavitating bubble populations: the nanodroplet injection model, J. Am. Chem. Soc. 131 (2009) 6060–6061.
[11] D.J. Flannigan, K.S. Suslick, Inertially confined plasma in an imploding bubble, Nat. Phys. 6 (2010) 598–601.
[12] K.S. Suslick, G.J. Price, Applications of ultrasound to materials chemistry, Annu. Rev. Mater. Sci. 29 (1999) 295–326.
[13] J.H. Bang, K.S. Suslick, Applications of ultrasound to the synthesis of nanostructured materials, Adv. Mater. 22 (2010) 1039–1059.
[14] R. Pecha, B. Gompf, Microimplosions: cavitation collapse and shock wave emission on a nanosecond time scale, Phys. Rev. Lett. 84 (2000) 1328–1330.
[15] T. Prozorov, R. Prozorov, K.S. Suslick, High velocity interparticle collisions driven by ultrasound, J. Am. Chem. Soc. 126 (2004) 13890–13891.
[16] S.J. Doktycz, K.S. Suslick, Interparticle collisions driven by ultrasound, Science 247 (1990) 1067–1069.
[17] W.T. Richards, A.L. Loomis, The chemical effects of high frequency sound waves I. A preliminary survey, J. Am. Chem. Soc. 49 (1927) 3086–3100.
[18] A. Kapustin, The effects of ultrasound on the kinetics of crystallization, 1963.
[19] C.T. Turner, T.T. Galkowski, W.F. Radle, A. VanHook, Grain formation by sonic irradiation, Int. Sugar J. 52 (1950) 298–299.
[20] J.R. Principe, D.M. Skauen, Preparation of microcrystalline progesterone using ultrasound, J. Pharm. Sci. 51 (1962) 389–390.
[21] R.M. Cohn, D.M. Skauen, Controlled crystallization of hydrocortisone by ultrasonic irradiation, J. Pharm. Sci. 53 (1964) 1040–1045.
[22] D.M. Skauen, Some pharmaceutical applications of ultrasonics, J. Pharm. Sci. 56 (1967) 1373–1385.
[23] S.L. Hem, The effect of ultrasonic vibrations on crystallization processes, Ultrasonics 5 (1967) 202–207.
[24] B. Ratsimba, B. Biscans, H. Delmas, J. Jenck, Sonocrystallization: the end of empiricism?, Kona Powder Part J. 17 (1999) 38–48.
[25] L.J. McCausland, P.W. Cains, P.D. Martin, Use the power of sonocrystallization for improved properties, Chem. Eng. Prog. 97 (2001) 56–61.
[26] R.D. Dennehy, Particle engineering using power ultrasound, Org. Process Res. Dev. 7 (2003) 1002–1006.
[27] G. Ruecroft, D. Hipkiss, T. Ly, N. Maxted, P.W. Cains, Sonocrystallization: the use of ultrasound for improved industrial crystallization, Org. Process Res. Dev. 9 (2005) 923–932.
[28] M.D.L. de Castro, F. Priego-Capote, Ultrasound-assisted crystallization (sonocrystallization), Ultrason. Sonochem. 14 (2007) 717–724.
[29] G. Cravotto, P. Cintas, Harnessing mechanochemical effects with ultrasound-induced reactions, Chem. Sci. 3 (2012) 295–307.
[30] Special issue on crystal growth and nucleation, Faraday Discuss. 136 (2007) 1–426.
[31] J. Anwar, D. Zahn, Uncovering molecular processes in crystal nucleation and growth by using molecular simulation, Angew. Chem. Int. Ed. 50 (2011) 1996–2013.
[32] J.W. Mullin, Crystallization, fourth ed., Butterworth-Heinemann, Oxford; Boston, 2001.
[33] H. Li, J.K. Wang, Y. Bao, Z.C. Guo, M.Y. Zhang, Rapid sonocrystallization in the salting-out process, J. Cryst. Growth 247 (2003) 192–198.
[34] Z. Guo, M. Zhang, H. Li, J. Wang, E. Kougoulos, Effect of ultrasound on anti-solvent crystallization process, J. Cryst. Growth 273 (2005) 555–563.
[35] M. Kurotani, E. Miyasaka, S. Ebihara, I. Hirasawa, Effect of ultrasonic irradiation on the behavior of primary nucleation of amino acids in supersaturated solutions, J. Cryst. Growth 311 (2009) 2714–2721.
[36] E. Miyasaka, Y. Kato, M. Hagisawa, I. Hirasawa, Effect of ultrasonic irradiation on the number of acetylsalicylic acid crystals produced under the supersaturated condition and the ability of controlling the final crystal size via primary nucleation, J. Cryst. Growth 289 (2006) 324–330.
[37] E. Miyasaka, S. Ebihara, I. Hirasawa, Investigation of primary nucleation phenomena of acetylsalicylic acid crystals induced by ultrasonic irradiation–ultrasonic energy needed to activate primary nucleation, J. Cryst. Growth 295 (2006) 97–101.
[38] K. Sangwal, Effect of impurities on the metastable zone width of solute-solvent systems, J. Cryst. Growth 311 (2009) 4050–4061.
[39] L. McCausland, P. Cains, Ultrasound to make crystals, Chem. Ind. (2003) 15–18.
[40] S. Gracin, M. Uusi-Penttila, A.C. Rasmuson, Influence of ultrasound on the nucleation of polymorphs of p-aminobenzoic acid, Cryst. Growth Des. 5 (2005) 1787–1794.
[41] M. Louhi-Kultanen, M. Karjalainen, J. Rantanen, M. Huhtanen, J. Kallas, Crystallization of glycine with ultrasound, Int. J. Pharm. 320 (2006) 23–29.
[42] M. Kurotani, I. Hirasawa, Polymorph control of sulfamerazine by ultrasonic irradiation, J. Cryst. Growth 310 (2008) 4576–4580.
[43] H. Hatakka, H. Alatalo, M. Louhi-Kultanen, I. Lassila, E. Haeggstrom, Closed-loop control of reactive crystallization part II: polymorphism control of L-glutamic acid by sonocrystallization and seeding, Chem. Eng. Technol. 33 (2010) 751–756.
[44] Y. Gong, B.M. Collman, S.M. Mehrens, E. Lu, J.M. Miller, A. Blackburn, D.J.W. Grant, Stable-form screening: overcoming trace impurities that inhibit solution-mediated phase transformation to the stable polymorph of sulfamerazine, J. Pharm. Sci. 97 (2008) 2130–2144.
[45] S.V. Dalvi, R.N. Dave, Controlling particle size of a poorly water-soluble drug using ultrasound and stabilizers in antisolvent precipitation, Ind. Eng. Chem. Res. 48 (2009) 7581–7593.
[46] S.V. Dalvi, R.N. Dave, Analysis of nucleation kinetics of poorly water-soluble drugs in presence of ultrasound and hydroxypropyl methyl cellulose during antisolvent precipitation, Int. J. Pharm. 387 (2010) 172–179.
[47] C. Beck, S.V. Dalvi, R.N. Dave, Controlled liquid antisolvent precipitation using a rapid mixing device, Chem. Eng. Sci. 65 (2010) 5669–5675.
[48] U.N. Hatkar, P.R. Gogate, Process intensification of anti-solvent crystallization of salicylic acid using ultrasonic irradiations, Chem. Eng. Process. 57–58 (2012) 16–24.
[49] O. Narducci, A.G. Jones, E. Kougoulos, An assessment of the use of ultrasound in the particle engineering of micrometer-scale adipic acid crystals, Cryst. Growth Des. 11 (2011) 1742–1749.
[50] O. Narducci, A.G. Jones, Seeding in situ the cooling crystallization of adipic acid using ultrasound, Cryst. Growth Des. 12 (2012) 1727–1735.
[51] R.K. Bund, A.B. Pandit, Sonocrystallization: effect on lactose recovery and crystal habit, Ultrason. Sonochem. 14 (2007) 143–152.
[52] R.S. Dhumal, S.V. Biradar, A.R. Paradkar, P. York, Ultrasound assisted engineering of lactose crystals, Pharm. Res. 25 (2008) 2835–2844.
[53] S.R. Patel, Z.V.P. Murthy, Ultrasound assisted crystallization for the recovery of lactose in an anti-solvent acetone, Cryst. Res. Technol. 44 (2009) 889–896.
[54] E. Kougoulos, I. Marziano, P.R. Miller, Lactose particle engineering: influence of ultrasound and anti-solvent on crystal habit and particle size, J. Cryst. Growth 312 (2010) 3509–3520.
[55] S.R. Patel, Z.V.P. Murthy, Optimization of process parameters by Taguchi method in the recovery of lactose from whey using sonocrystallization, Cryst. Res. Technol. 45 (2010) 747–752.
[56] S.R. Patel, Z.V.P. Murthy, Effect of process parameters on crystal size and morphology of lactose in ultrasound-assisted crystallization, Cryst. Res. Technol. 46 (2011) 243–248.
[57] S.R. Patel, Z.V.P. Murthy, Lactose recovery processes from whey: a comparative study based on sonocrystallization, Sep. Purif. Rev. 41 (2012) 251–266.
[58] P.J. Gandhi, Z.V.P. Murthy, Solubility and crystal size of sirolimus in different organic solvents, J. Chem. Eng. Data 55 (2010) 5050–5054.
[59] P.J. Gandhi, Z.V.P. Murthy, Kinetic study of ultrasonic antisolvent crystallization of sirolimus, Cryst. Res. Technol. 45 (2010) 321–327.
[60] P.J. Gandhi, Z.V.P. Murthy, R.K. Pati, Optimization of process parameters by Taguchi robust design method for the development of nano-crystals of sirolimus using sonication based crystallization, Cryst. Res. Technol. 47 (2012) 53–72.
[61] M.W. Park, S.D. Yeo, Antisolvent crystallization of roxithromycin and the effect of ultrasound, Sep. Purif. Rev. 45 (2010) 1402–1410.

[62] M.W. Park, S.D. Yeo, Antisolvent crystallization of carbamazepine from organic solutions, Chem. Eng. Res. Des. 90 (2012) 2202–2208.
[63] J.R.G. Sander, D.K. Bučar, R.F. Henry, G.G.Z. Zhang, L.R. MacGillivray, Pharmaceutical nano-cocrystals: sonochemical synthesis by solvent selection and use of a surfactant, Angew. Chem. Int. Ed. 49 (2010) 7284–7288.
[64] V.S. Nalajala, V.S. Moholkar, Investigations in the physical mechanism of sonocrystallization, Ultrason. Sonochem. 18 (2011) 345–355.
[65] J. Lee, M. Ashokkumar, S.E. Kentish, Influence of mixing and ultrasound frequency on antisolvent crystallisation of sodium chloride, Ultrason. Sonochem. 21 (2014) 60–68.
[66] A. Kordylla, S. Koch, F. Tumakaka, G. Schembecker, Towards an optimized crystallization with ultrasound: effect of solvent properties and ultrasonic process parameters, J. Cryst. Growth 310 (2008) 4177–4184.
[67] K. Wohlgemuth, F. Ruether, G. Schembecker, Sonocrystallization and crystallization with gassing of adipic acid, Chem. Eng. Sci. 65 (2010) 1016–1027.
[68] S. Nii, S. Takayanagi, Growth and size control in anti-solvent crystallization of glycine with high frequency ultrasound, Ultrason. Sonochem. 21 (2014) 1182–1186.
[69] K. Wohlgemuth, A. Kordylla, F. Ruether, G. Schembecker, Experimental study of the effect of bubbles on nucleation during batch cooling crystallization, Chem. Eng. Sci. 64 (2009) 4155–4163.
[70] A. Kordylla, T. Krawczyk, F. Tumakaka, G. Schembecker, Modeling ultrasound-induced nucleation during cooling crystallization, Chem. Eng. Sci. 64 (2009) 1635–1642.
[71] K. Wohlgemuth, G. Schembecker, Modeling induced nucleation processes during batch cooling crystallization: a sequential parameter determination procedure, Comput. Chem. Eng. 52 (2013) 216–229.
[72] J. Dodds, F. Espitalier, O. Lonisnard, R. Grossier, R. David, M. Hassoun, F. Baillon, C. Gatumel, N. Lyczko, The effect of ultrasound on crystallisation-precipitation processes: some examples and a new segregation model, Part. Part. Syst. Char. 24 (2007) 18–28.
[73] B.W. Zeiger, K.S. Suslick, Sonofragmentation of molecular crystals, J. Am. Chem. Soc. 133 (2011) 14530–14533.
[74] V.B. Patravale, A.A. Date, R.M. Kulkarni, Nanosuspensions: a promising drug delivery strategy, J. Pharm. Pharmacol. 56 (2004) 827–840.
[75] J.S. Patton, P.R. Byron, Inhaling medicines: delivering drugs to the body through the lungs, Nat. Rev. Drug Dis. 6 (2007) 67–74.
[76] N. El-Gendy, E.M. Gorman, E.J. Munson, C. Berkland, Budesonide nanoparticle agglomerates as dry powder aerosols with rapid dissolution, J. Pharm. Sci. 98 (2009) 2731–2746.
[77] N. El-Gendy, P. Selvam, P. Soni, C. Berkland, Development of budesonide nanocluster dry powder aerosols: processing, J. Pharm. Sci. 101 (2012) 3425–3433.
[78] N. El-Gendy, P. Selvam, P. Soni, C. Berkland, Development of budesonide nanocluster dry powder aerosols: preformulation, J. Pharm. Sci. 101 (2012) 3434–3444.
[79] N. El-Gendy, S. Huang, P. Selvam, P. Soni, C. Berkland, Development of budesonide nanocluster dry powder aerosols: formulation and stability, J. Pharm. Sci. 101 (2012) 3445–3455.
[80] R.S. Dhumal, S.V. Biradar, A.R. Paradkar, P. York, Particle engineering using sonocrystallization: salbutamol sulphate for pulmonary delivery, Int. J. Pharm. 368 (2009) 129–137.
[81] Y.T. Song, W.C. Chen, X.L. Chen, Ultrasonic field induced chiral symmetry breaking of NaClO3 crystallization, Cryst. Growth Des. 8 (2008) 1448–1450.
[82] P. Cintas, On cavitation and chirality: a further assessment, Cryst. Growth Des. 8 (2008) 2626–2627.
[83] Y.T. Song, W.C. Chen, X.L. Chen, Crystal chiral symmetry breaking: a self-seed inducing effect controlled by kinetics, Cryst. Growth Des. 12 (2012) 8–11.
[84] D.K. Bučar, L.R. MacGillivray, Preparation and reactivity of nanocrystalline cocrystals formed via sonocrystallization, J. Am. Chem. Soc. 129 (2007) 32–33.
[85] C. Karunatilaka, D.K. Bučar, L.R. Ditzler, T. Friščić, D.C. Swenson, L.R. MacGillivray, A.V. Tivanski, Softening and hardening of macro- and nano-sized organic cocrystals in a single-crystal transformation, Angew. Chem. Int. Ed. 50 (2011) 8642–8646.
[86] D.P. Yan, D.K. Bučar, A. Delori, B. Patel, G.O. Lloyd, W. Jones, X. Duan, Ultrasound-assisted construction of halogen-bonded nanosized cocrystals that exhibit thermosensitive luminescence, Chem. Eur. J. 19 (2013) 8213–8219.
[87] J.S. Kaerger, R. Price, Processing of spherical crystalline particles via a novel solution atomization and crystallization by sonication (SAXS) technique, Pharm. Res. 21 (2004) 372–381.
[88] A.B.D. Antunes, B.G. De Geest, C. Vervaet, J.P. Remon, Solvent-free drug crystal engineering for drug nano- and micro suspensions, Eur. J. Pharm. Sci. 48 (2013) 121–129.